Fate of US and Canadian combustion nitrogen emissions

Hiram Levy II & Walter J. Moxim

Geophysical Fluid Dynamics Laboratory/NOAA, Princeton University, PO Box 308, Princeton, New Jersey 08542, USA

While approximately 7.5×10^{12} grams (7.5 Tg) of combustion nitrogen are emitted yearly in the United States and Canada[1-3], only 1.5–2.3 Tg are deposited as acid rain over that same region[4-6]. Past nitrogen budget estimates[4,10] as well as recent observations[11] suggest that dry deposition and export play major roles. Here we report how the yearly accumulated deposition and transport of combustion nitrogen is simulated for the first time by a global transport model with realistic meteorology. The model predicts that dry deposition over the United States and Canada accounts for at least 2.1 and most probably 3.5 Tg of the emissions. The remainder is exported, principally over the North Atlantic. But at most 0.2 Tg, less than 3% of the estimated European emissions[4], is predicted to reach Europe from North America. Furthermore, the model predicts that, while less than 40% of the nitrogen deposited as acid rain in the northeastern United States and eastern Canada comes from emissions in that region, almost all of the dry-deposited nitrogen and over half of the total acid nitrogen deposition comes from there.

Rather than simulations of individual storms and their resulting deposition and transport[9], we are interested in the accumulated impact of nitrogen emissions. The Geophysical Fluid Dynamics Laboratory (GFDL) general circulation/transport model has 11 terrain-following levels with standard heights of 31.4, 22.3, 18.8, 15.5, 12.0, 8.7, 5.5, 3.1, 1.5, 0.5, 0.08 km, a horizontal grid size of ~265 km, and a time step of ~26 min. The 6-h time average winds and precipitation provided by the parent general circulation model compare well with observed global climatology[7,8]. This model also generates an ensemble of realistic weather patterns over North America that mimic real synoptic systems in their structure and evolution (W.J.M. & H.L.II, in preparation).

The gaseous and particulate nitrogen compounds resulting from both direct emissions and chemical transformations make up the collection of reactive nitrogen compounds that we call NO_y. These compounds are transported as a single tracer and satisfy the following continuity equation:

$$\frac{\partial R p_*}{\partial t} = \text{TRANSPORT} + \text{SOURCE} - D p_* R - \Phi p_* R \quad (1)$$

In equation (1) R is the NO_y volume mixing ratio, p_* is the surface pressure, D is the dry deposition coefficient, and Φ is the precipitation removal coefficient. The formulation of TRANSPORT, which represents flux convergence resulting from both the resolved air motions and sub-grid scale diffusion, is described in detail elsewhere[12-14].

SOURCE is constructed from yearly average point and area emission inventories[1,2] and held constant throughout the year. It includes an apportionment of point sources by stack height (ref. 3; A. Kosteltz, personal communication). Integrated over the source region, 65% of the emissions enter at the model surface, 20% at the middle of the bottom level (80 m) and 15% are injected into the second level at a standard height of 500 m. The distribution of total yearly emissions is shown in Fig. 1. The cross-hatched area, running northwards and eastwards from central Pennsylvania, delineates the source for the northeastern United States and eastern Canada and contains 15% of the total nitrogen emissions.

Chemical reactions[15], by oxidizing insoluble nitrogen oxides to soluble nitric acid and by apportioning NO_y among the nitrogen compounds with their differing deposition velocities, control the rate of acid deposition. However, chemical reactions only enter our model implicitly via the bulk removal coefficients, D and Φ, discussed next. This is equivalent to assuming that the chemical partitioning is rapid relative to transport. While valid near the surface where the chemistry and removal are generally fast, this assumption starts to break down in the middle troposphere where the reactions can be much slower.

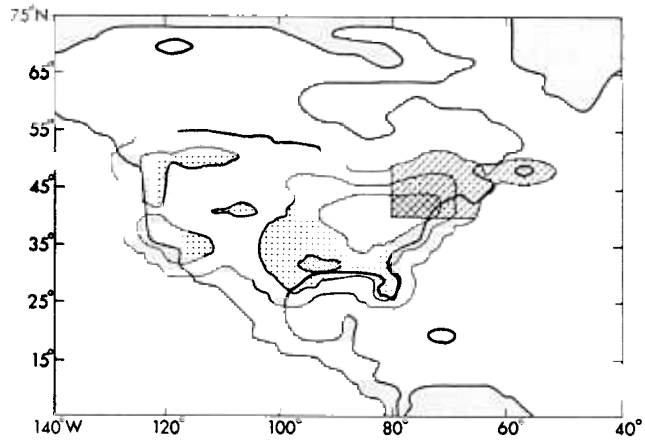

Fig. 1 Yearly total combustion nitrogen source (mmol m^{-2} yr^{-1}) for the United States and Canada. ☐ 0–20 mmol m^{-2}; ⬚ 20–100 mmol m^{-2}; ▩ 100 mmol m^{-2}; ■ North-east region.

Table 1 Combustion nitrogen budget for the United States and Canada

Simulation w_{eff} +	N	Acid precipitation (% of emissions)	Dry deposition (% of emissions)	Export (% of emissions)
0.3 cm s^{-1}	9	28%	46%	26%
0.1 cm s^{-1}	5	29%	28%	43%

Dry deposition, a continuous process occurring only at the surface, is expressed as a first-order loss term in equation (1). The coefficient D is given in equation (2) of ref. 14 with w_0 replaced by an effective deposition velocity,

$$w_{eff} = \frac{1}{R_{11}(NO_y)} \sum_i R_{11}(i) w(i) \quad (2)$$

that depends on the chemical partitioning of NO_y. $R_{11}(i)$ is the volume mixing ratio of the ith reactive nitrogen species in the lowest level and $w(i)$ is its measured deposition velocity. For a more detailed discussion, see refs 17 and 18. Using available measurements of $w(i)$ and $R(i)$[4,16-20], we find that, while values of both vary greatly with time and location, w_{eff} over land ranges from 0.6 cm s^{-1} in the summer to 0.2 cm s^{-1} in the winter.

With no chemical scheme in the model to calculate w_{eff}, we treat it as a parameter. Because we are primarily interested in yearly dry deposition, constant values, 0.3 cm s^{-1} over land and 0.1 cm s^{-1} over the ocean, are selected from the low end of the seasonal range. To determine the sensitivity of our conclusions to the variability and uncertainty in w_{eff}, simulations are also performed for $w_{eff} = 1.0$ cm s^{-1}, an upper limit which assumes that HNO_3 is the principal nitrogen compound, and for $w_{eff} = 0.1$ cm s^{-1}, a lower limit which assumes that $HNO_3 = 0.1 NO_y$ and the ground is snow-covered.

Precipitation removal, an intermittent process acting throughout the tropospheric column, is also expressed as a first-order loss term in equation (1). The removal coefficient at level k, Φ_k, is given by

$$\Phi_k = N B_k [\text{Rain}/\text{Rain}^G] \quad (3)$$

where Rain is the 6-h model precipitation at a given surface

Table 2 Comparison of observations and simulations for selected stations

Station	Precipitation cm yr^{-1}		Acid nitrogen precipitation mmol m^{-2} yr^{-1}		
	Model	Observed	$w_{eff} = 0.3$	Observed	$w_{eff} = 0.1$
Oak Ridge TN	76	128	18	21	18
Oxford OH	62	98	23	24	23
Urbana IL	51	88	25	22	24
Charlottesville VA	89	106	33	25	34
State College PA	107	109	34	33	37
Ithaca NY	113	104	40	30	44
Chalk River Ont.	93	80	27	24	29
Whiteface NY	129	111	41	21	44
Lewes DE	107	118	26	22	27
Brookhaven NY	117	116	46	22	46
Bermuda	190	172	5	6	6
Nova Scotia	125	140	18	14	20
Bay D'Espoir Nfld	103	165	10	9	12
Montmorency Que	128	116	27	25	30
Goose Bay Nfld	140	94	11	7	15

grid box, $Rain^G$ is the global average for the same period, $1/B_k$ is a lifetime based on the vertical distribution of rainfall[12] and ranges from 20 days at the lowest level to 60 days at the 8.7 km level. The parameter, N represents the effective solubility of the trace species. The deposition of radioactive debris from nuclear tests in the stratosphere[12] has been successfully simulated with $N = 1$. A formulation for highly soluble gases, based on Henry's Law of solubility and a parameterization of cloud physics that includes both rainout in the cloud and washout below the cloud, reduces to a form similar to equation (3) (W.L.C., H.L.II and W.J.M., in preparation). Here, N depends on the fraction of NO_y present as gaseous HNO_3 at the onset of precipitation and on the rate of conversion of insoluble nirogen oxides to highly soluble nitric acid during the precipitation event. While the model has no chemical scheme to calculate the fraction and conversion rate, the percentage of emissions deposited yearly in acid rain over the United States and Canada is known (25%–30%[4-6]). The parameter N is set to bring the simulated yearly acid rain into this range. Based on recent observations[24], we include no seasonal dependence. Since the level of NO_y increases with decreasing w_{eff} and the deposition of acid rain is fixed, the chosen value for N will decrease with w_{eff}. While the area integral depends on N, the spatial pattern of deposition as well as individual station values depend on the transport model's meteorology.

Fifteen-month simulations with the US-Canadian source, all using the same meteorology, were completed for three values of w_{eff} over land (1.0, 0.3, and 0.1 cm s^{-1}) with N set at 18, 9, and 5 respectively. The apportionment of the combustion nitrogen emission among acid precipitation, dry deposition and export is given in Table 1 for the last two simulations. At the lower limit for w_{eff} (0.1 cm s^{-1}), dry deposition still equals deposition in acid rain. While export becomes the major term in the budget, only 3% of the emissions reach Europe. For the more probable value of w_{eff} (0.3 cm s^{-1}), dry deposition is the dominant term in the budget. The major portion of exported nitrogen is still carried out over the North Atlantic, though now only 1% of the emissions reaches Europe. Less than 0.1% survives the tropical rainbelt to reach the southern hemisphere. While these results confirm the qualitative correctness of earlier estimates[4,10], our simulation, using the more probable value of w_{eff}, predicts dry deposition that is significantly higher than earlier estimates and export from the continent that is at the lower bound of past estimates. In particular, a realistic meteorological model transports much less to Europe than does a model driven by seasonal mean winds[10].

The upper limit for w_{eff} [1.0 cm s^{-1}] requires that over half of the NO_y exist as HNO_3 and results in complete domination of the nitrogen budget by dry deposition. The resulting surface concentrations of NO_y are much less than observed, and an unrealistically high value of N is needed to even approach the observed deposition in acid rain.

Simulations of yearly precipitation and its nitrogen content for w_{eff} set at 0.3 and 0.1 cm s^{-1} over land are compared in Table 2 with observations from a selection of United States and Canadian stations[21-23,25]. The spatial pattern and most of the individual stations are in good agreement with observations. The model's dryness in the mid-west leads to a slight underestimate of acid rain there and similarly the excess precipitation in the far north-east leads to a slight overestimate. The three stations that are significantly higher than observed (Ithaca, Whiteface and Brookhaven) are all relatively unpolluted sites near regions of high emissions for which the model's 265-km grid resolution is not sufficient. The last five stations in Table 2 represent export to the North Atlantic. The predicted export to Bermuda is a little low but it is quite good for the Maritimes and northern Quebec.

While the model's grid resolution is too coarse to resolve areas of low emission embedded in or near regions of significant combustion, it is adequate to resolve a regional source embedded in North America (cross-hatched area in Fig. 1). We shut off 85% of the combustion nitrogen source and leave it on in 16 grid-boxes in the northeastern United States and eastern Canada. The simulation is then run for 15 months with our most realistic estimate for w_{eff} (0.3 cm s^{-1}) and its companion value $N = 9$. By comparing the deposition over the northeastern United States and eastern Canada from this simulation with that from the previous one using the complete combustion source, we can determine the relative importance of regional and distant sources to acid rain, dry deposition and total deposition of acid nitrogen in the region. The various contributions are shown in Table 3. Acid rain in the north-east is dominated by emissions transported from distant sources, while dry deposition comes overwhelmingly from emissions in the north-east. Over half of the total accumulation of acidic nitrogen is a result of local and regional emissions. While acid rain and dry deposition are comparable over the region as a whole, dry deposition dominates in the northeastern United States and the populated regions of eastern Canada. Only in northern Canada far from major sources, do acid rain and transport from distant sources dominate.

Table 3 Nitrogen deposition in the northeastern United States and eastern Canada

Emission source	Acid precipitation (Tg(N)yr^{-1})	Dry deposition (Tg(N)yr^{-1})	Total deposition (Tg(N)yr^{-1})
Regional	0.28	0.48	0.76
Distant	0.50	0.13	0.63

Given these results, we conclude that the current acid rain networks in the United States and Canada measure less than half of the acidic nitrogen that is accumulating in the environment, and that the current monitoring programme in the north-eastern United States and eastern Canada exaggerates the role of transport from the mid-west, south-east and Ohio Valley and underestimates the importance of local and regional emissions. Given this apparent major role for dry deposition, it is important that we determine its impact on the acidification of the environment.

We wish to acknowledge the many helpful comments of S. Manabe, J. D. Mahlman and J. N. Galloway.

Received 11 February; accepted 5 May 1987.

1. *1982 National Emissions Report, National Emissions Data System* US Environmental Protection Agency Report (Environmental Protection Agency, Research Triangle Park, NC, 1984).
2. *A Nationwide Inventory of Emissions of Air Contaminants (1976)*, Environmental Protection Service Report, Environmental Protection Service, Ottawa, Ontario, 1981).
3. Toothman, D. A., Yates, J. C. & Sabo, E. J. *Status Report on the Development of the NAPAP Emission Inventory for the 1980 Base Year and Summary of Preliminary data* (Environmental Protection Agency, Research Triangle Park, NC, 1984).
4. Logan, J. *J. geophys. Res.* **88**, 10785-10807 (1983).
5. Golomb, D. *Atmos. Environ.* **17**, 1387-1390 (1983).
6. Barrie, L. A. & Hales, J. M. *Tellus* **36B**, 333-355 (1984).
7. Manabe, S. Hahn, D. G. & Holloway, J. L. Jr *J. atmos. Sci.* **31**, 43-83 (1974).
8. Manabe, S. & Holloway, J. L. Jr *J. geophys. Res.* **80**, 1617-1649 (1975).
9. Chang, J. S. *et al. J. geophys. Res.* (in the press).
10. Galloway, J. N., Whelpdale, D. M. & Wolff, G. T. *Atmos. Environ.* **18**, 2595-2607 (1984).
11. Lindberg, S. E., Lovett, G. M., Richter, D. D. & Johnson, D. W. *Science* **231**, 141-145 (1986).
12. Mahlman, J. D. & Moxim, W. J. *J. atmos. Sci.* **35**, 1340-1374 (1978).
13. Levy, H. II, Mahlman, J. D. & Moxim, W. J. *J. geophys. Res.* **87**, 3061-3080 (1982).
14. Levy, H. II, Mahlman, J. D., Moxim, W. J. & Liu, S. C. *J. geophys. Res.* **90**, 3753-3772 (1985).
15. Stockwell, W. R. *Atmos. Environ.* **20**, 1615-1632 (1986).
16. Fahey, D. W. *et al. J. geophys. Res.* **91**, 9781-9793 (1986).
17. Walcek, C. J., Brost, R. A., Chang, J. S. & Wesely, M. L. *Atmos. Environ.* **20**, 949-964 (1986).
18. Voldner, E. C.,Barrie, L. A. & Sirois, A. *Atmos. Environ.* **20**, 2101-2123 (1986).
19. Cadle, S. H., Dasch, J. M. & Mulawa, P. A. *Atmos. Environ.* **19**, 1819-1827 (1985).
20. Garland, J. A. & Penkett, S. A. *Atmos. Environ.* **10**, 1127-1131 (1976).
21. Dana, M. T. & Easter, R. C. *Atmos. Environ.* (in the press).
22. Vet, R. J., Sukoff, W. B., Still, M. E. & Gilbert, R. *CAPMoN Precipitation Chemistry Data Summary 1983-1984* (Atmospheric Environment Service, Downsview, Ontario, 1986).
23. Summers, P. W., Bowersox, V. C. & Stensland, G. J. *J. Water, Air Soil Pollut* (in the press).
24. Summers, P. W. & Barrie, L. A. *J. Water, Air Soil Pollut.* (in the press).
25. Galloway, J. N., Artz, R. S., Keene, W. Z., Church, T. M. & Knapp, A. H. *J. geophys. Res.* (submitted).

Six-coordinated silicon in glasses

R. Dupree, D. Holland & M. G. Mortuza

Centre for Advanced Materials Technology, Department of Physics, Warwick University, Coventry CV4 7AL, UK

It has been accepted since 1932 that the building block of silicate glasses consists of silicon tetrahedrally coordinated to 4 oxygen atoms[1]. Although the existence of 6-coordinated silicon in a few crystalline materials, such as stishovite, and SiP_2O_7 is known[2,3], the presence of (SiO_6) units has not yet been observed experimentally in glasses. Recent X-ray diffraction and magic-angle-spinning (MAS) nuclear magnetic resonance investigations[4,5] of SiO_2-P_2O_5 glasses found only 4-coordinated silicon although SiP_2O_7 was produced by devitrification. Raman studies[6] of Na_2O-SiO_2-P_2O_5 glasses were interpreted as indicating the presence of a structural unit containing Si-O-P bonding but otherwise unidentifiable. We have applied MAS nuclear magnetic resonance spectroscopy to similar glasses and here we report the first observation of [SiO_6] units in glasses.

Sodium disilicate base glasses NSP1-NSP4, with different amounts of phosphorus as given in Table 1, were prepared from mixtures of analytical grade diammonium hydrogen phosphate, silica and sodium carbonate. The glass batch was preheated at 200 °C for 1.5 h to volatilize NH_3 and H_2O and then melted in alumina crucibles at 1,575 °C for 4 hours (NSP1) or 1,100 °C for 2.5 h (NSP2, 3, 4). All samples were splat-cooled between two graphite coated steel plates at room temperature and were subsequently stored in a desiccator. $MnCO_3$ at 0.05 mol % was added to each batch to reduce the ^{29}Si relaxation time, since this is typically 10 min in undoped samples. Control experiments on undoped samples showed that there was no difference in relative peak intensities due to small additions of $MnCO_3$. All MAS nuclear magnetic resonance (NMR) spectra were recorded on a Bruker MSL 360 spectrometer operating at ~71.5 MHz for ^{29}Si and 145.8 MHz for ^{31}P nuclei. The delays between pulses were chosen by increasing the relaxation delay until the relative intensities from different species did not alter. Typically 2-μs ($\sim\pi/6$) pulses with a 60-s delay were used for acquiring ^{29}Si spectra and 4 μs ($\sim\pi/2$) pulses with 1 s delay for ^{31}P. Chemical shifts were measured relative to tetramethylsilane, 85% H_3PO_4 and dilute aqueous NaCl for ^{29}Si, ^{31}P and ^{23}Na respectively. As some contamination from the alumina crucibles was anticipated, ^{27}Al spectra were also acquired with aqueous $Al(NO_3)_3$ as reference. From the size of the ^{27}Al signal and also from dispersive X-ray energy analysis, the level of contamination was estimated to be 2 mol %. Glasses NSP2-4 were transparent and X-ray amorphous. However, in NSP1, sporadic nucleation was observed but the clear portions of the glass selected for NMR experiments were shown to be X-ray amorphous within the detection limit of X-ray diffraction, that is significantly less than 5% crystalline. The spectra recorded for ^{29}Si and ^{31}P are illustrated in Figs 1 and 2 and the isotropic peak positions, halfwidths and relative intensities are recorded in Table 1.

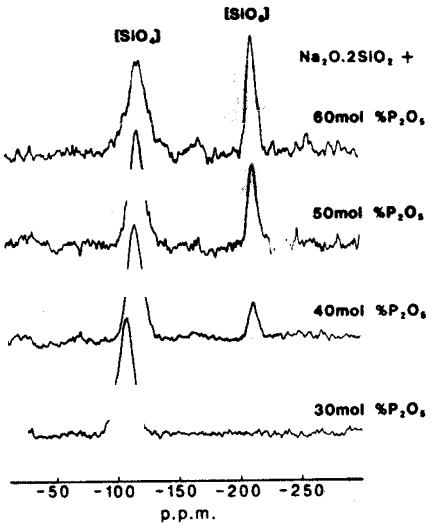

Fig. 1 MAS-NMR spectra of ^{29}Si in sodium disilicate glasses containing 30, 40, 50 and 60 mole % P_2O_5. Approximately 0.4 g of sample were used in Delrin rotors which were spun at 3.0-3.5 kHz.

We have recently reported[7] that the addition of small amounts (1-5 mol %) of P_2O_5 to alkali disilicate glasses results in the scavenging of modifier cations by phosphorus to give orthophosphate M_3PO_4 and pyrophosphate $M_4P_2O_7$ units accompanied by polymerization of the silicate network, that is, elimination of non-bridging oxygens and conversion of Q^3 $Si(OSi)_3O^-$ to Q^4 $Si(OSi)_4$ silicons. The phosphorus thus appears to play no part in the glass network at these concentrations. Above ~10 mole % P_2O_5, glass formation is difficult because of high liquidus temperatures but becomes easier beyond 30 mol % P_2O_5. Up to 30 mol % P_2O_5 we observe increasing polymerization of the phosphate groups, first to give pyrosphate dimers, then metaphosphate chains and the silicon spectra show the presence of Q^4 only. However, the MAS spectra obtained from glasses of >30 mol % P_2O_5 content are now most unusual. In the 30 mol % P_2O_5 glass (NSP1) a single peak is observed in the ^{29}Si spectrum at −109 p.p.m., characteristic of pure Q^4 as in vitreous SiO_2 undiluted by other species. The ^{31}P spectrum also contains a single resonance (plus associated side bands) at −16 p.p.m. which is characteristic of metaphosphate $(NAPO_3)_n$